Astron. Astrophys. 331, 1078–1086 (1998)

ASTRONOMY
AND
ASTROPHYSICS

Slow and fast magnetic reconnection

I. Role of radiative cooling

A.V. Oreshina and B.V. Somov

Solar Physics Department, Astronomical Institute, Moscow State University, Universitetskii Prospekt 13, Moscow 119899, Russia
(e-mail: somov@sai.msu.su)

Received 30 July 1997 / Accepted 13 November 1997

Abstract. New model of a magnetically non-neutral reconnecting current sheet (RCS) in the solar corona is developed to investigate different structures of the RCS and different regimes of reconnection corresponding to these structures. In this paper (Paper 1) we formulate the mathematical problem and consider mainly the solutions that demonstrate an influence of the radiative cooling on the RCS structure and reconnection rate. The solution for low temperatures ($T \sim 10^4$ K) of plasma in the RCS, when heat conduction is not important, shows that the radiative losses of energy make the current sheet be thinner, denser, and colder; the velocity of plasma outflows from it slows down. The transition from the slow regime of reconnection (with the magnetic field configuration of O-type in a central region of the RCS) to the fast one (with the configuration of X-type) is realized at larger rates of reconnection as compared with the case where radiation is not taken into account. This result makes more probable the formation of solar prominences via slow magnetic reconnection in the RCS with magnetic island in the central region of current sheet. The transition from slow reconnection to fast one presumably means destabilization of a quiescent prominence and triggering a flare.

Key words: magnetohydrodynamics – Sun: corona – Sun: magnetic fields – Sun: prominences

1. Introduction

It is widely believed that magnetic reconnection plays a key role in dynamics of astrophysical plasmas, especially in solar flares (Giovanelli 1946; Hones 1984). Reconnection serves as a highly efficient engine to convert magnetic energy into thermal and kinetic energies of plasma flows and accelerated particles (e.g., Syrovatskii 1966; Somov 1994). However, before the *Yohkoh* satellite (Ogawara et al. 1991), there were no direct clear evidence that magnetic reconnection is responsible for the primary release of flare energy.

Solar hard and soft X-ray observations (Kosugi et al. 1991; Tsuneta et al. 1991) on board *Yohkoh* suggest that magnetic reconnection is responsible for many non-steady phenomena in the corona (e.g., Uchida et al. 1996). In particular, in many solar flares the reconnection of magnetic field lines takes place. Reconnection seems to be common to impulsive (compact) and gradual (large-scale) flares. However, in the interpretation of the *Yohkoh* data, 'the basic physics of the reconnection process remains uncertain' (Masuda et al. 1994; see also Sect. 8 in Kosugi and Somov 1997).

Following the two-dimensional (2D) magnetohydrodynamic (MHD) 'standard model' of a two-ribbon flare (Forbes & Priest 1982, 1983; see also references in Tsuneta 1996), the reconnecting current sheet (RCS) in flares is considered as a 'point' which is responsible to the reconnection process only in geometrical sense, i.e. the X-type point at which connectivity of field lines in a 2D plane changes (Masuda et al. 1995; Forbes & Acton 1996; Tsuneta 1996; Tsuneta et al. 1997). Just like in the vacuum or in a plasma of very low conductivity, it is supposed that no energy is converted by this point. External hydrodynamics in the vicinity of the X-type point is discussed and is numerically simulated in terms of slow MHD shock waves. They convert the energy of interacting magnetic fluxes into thermal and kinetic energy of fast flows of hot plasma. It means, in fact, that the well known Petschek model of the reconnection process (Petschek 1964) is used to explain energetics and dynamics of plasma flows in solar flares.

According to this model, four slow MHD shock waves depart from the X-point. In these waves, the slow flows of plasma toward the X-point in one pair of opposite sectors are transformed into fast flows away from the X-point in the other pair of sectors. The immediate vicinity of the X-point is the so-called 'diffusion region', in which the magnetic field lines of the two oppositely directed plasma flows are reconnected.

Contrary to the well established opinion, the Petschek diffusion region differs from the so-called 'neutral sheet' or, more exactly, magnetically neutral current sheet – the RCS without any internal magnetic field (e.g., Sweet 1969, Syrovatskii 1971) – in two physical regards. First, the current density at the center

of the diffusion region is minimal, while that at the center of the neutral sheet is maximal. Second, as the plasma conductivity increases, the width of the diffusion region decreases (see Eq. (20) in Petschek 1964), while the width of the neutral sheet increases. This difference appears from different mechanisms of magnetic energy conversion.

Another principal distinction between the neutral sheet and the Petschek MHD flow lies in the nature of the boundary conditions (Syrovatskii 1976a). Only in recent years has the basic inconsistency of the Petschek model become apparent (see Sect. 6 in Biskamp 1993; see also Biskamp 1986).

In general, numerical MHD simulations of the magnetic reconnection process demonstrate co-existance of a *thin but wide* current sheet with fast (or slow) shock waves attached to the edges of the RCS (e.g., Brushlinskii, Zaborov, & Syrovatskii 1980; Podgorny and Syrovatskii 1981; Forbes and Priest 1983) or to the return-current regions (e.g., Biskamp 1993; Hesse et al. 1996). Hydrodynamics of the external plasma flows in the RCS vicinity strongly depends, of course, on the boundary and initial conditions (e.g., Priest and Lee 1990). That is why we give preference to the physics of magnetic reconnection – the self-consistent treatment of the RCS rather than that of the external hydrodynamics.

In the present paper (Paper 1) we investigate the problem on the structure of the current sheet and look for conditions of forming a 'magnetic island' – region of closed magnetic lines – in the center of the RCS, and also conditions under which a magnetic configuration of X-type forms. This model is an extension of the previous study (Sect. 3.4 in Somov 1992); an emphasis is placed on the role of radiative losses.

A plan of the paper is as follows. In Sect. 2, we formulate a mathematical problem: a set of MHD equations is written, some needful functions are postulated, and boundary conditions are set. Basic stages of the solving procedure are outlined in Sect. 3 because they are not trivial. Further results of numerical computations are presented. The model taking into account the radiative losses is compared with that one without losses (Sect. 4). Discussion of results and comparison them with the previous works devoted to the current sheet equilibrium and structure are made briefly in Sect. 5. As an addition, a numerical method used for solving the system of equations is described in Appendix.

2. Mathematical description of the model

A stationary dissipative 2D MHD problem is considered (see Fig. 1). We use the following equations (with usual designations):

(1) the continuity equation

$$\mathrm{div}\,(\rho\,\boldsymbol{v}) = 0\,; \tag{1}$$

(2) the equation of energy conservation (with the radiative cooling)

$$-\mathrm{div}\,\boldsymbol{G} - \mathscr{L} = 0\,, \tag{2}$$

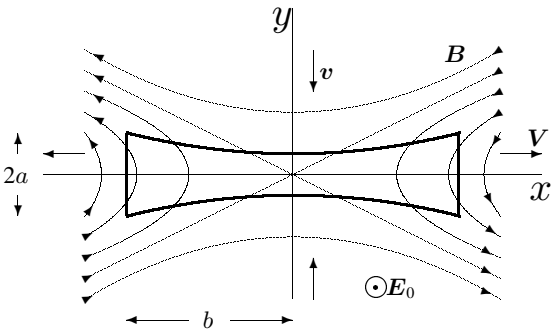

Fig. 1. The model of a thin wide reconnecting current sheet

where

$\boldsymbol{G} = \rho\,\boldsymbol{v}\,(\frac{v^2}{2} + w) + \boldsymbol{S}$ – energy flux density,

$w = \frac{5}{2}\,\frac{p}{\rho}$ – specific enthalpy,

$\boldsymbol{S} = \frac{c}{4\,\pi}\,[\boldsymbol{E} \times \boldsymbol{B}]$ – Poynting's vector,

$\mathscr{L}\,(T,\, n_{\mathrm{e}},\, n)$ – radiative loss function;

(3) the equation of momentum conservation

$$\frac{\partial}{\partial\, r_\beta}\,\Pi^*_{\alpha\,\beta} = 0 \quad \Rightarrow \quad \begin{cases} \dfrac{\partial}{\partial\, x}\,\Pi^*_{x\,x} + \dfrac{\partial}{\partial\, y}\,\Pi^*_{x\,y} = 0\,, \\ \dfrac{\partial}{\partial\, x}\,\Pi^*_{y\,x} + \dfrac{\partial}{\partial\, y}\,\Pi^*_{y\,y} = 0\,, \end{cases} \tag{3}$$

where $\Pi^*_{\alpha\,\beta}$ – tensor of momentum flux density,

$$\Pi^*_{\alpha\,\beta} = p\,\delta_{\alpha\,\beta} + \rho\,v_\alpha\,v_\beta + \frac{1}{4\,\pi}\,\left(\frac{B^2}{2}\,\delta_{\alpha\,\beta} - B_\alpha\,B_\beta\right)\,,$$

$$\delta_{\alpha\,\beta} = \begin{cases} 1, & \text{if } \alpha = \beta, \\ 0, & \text{if } \alpha \neq \beta; \end{cases}$$

(4) Ohm's law

$$\boldsymbol{j} = \sigma\,\{\boldsymbol{E} + \frac{1}{c}\,[\boldsymbol{v} \times \boldsymbol{B}]\}\,; \tag{4}$$

(5) Maxwell's equations

$$\mathrm{rot}\,\boldsymbol{B} = \frac{4\,\pi}{c}\,\boldsymbol{j}\,; \tag{5}$$

$$\mathrm{div}\,\boldsymbol{B} = 0\,. \tag{6}$$

Then we assume that the thickness $2a$ of the current sheet (Fig. 1) depends only on the coordinate x and remains much smaller than its width $2b$. This approach allows us to consider the current sheet as a whole along the y direction. Therefore, the problem becomes quasi-one-dimensional, i.e. all unknown functions, describing the current sheet, depend on the coordinate x only.

Eqs. (1)–(4) are integrated over the thickness of the sheet, i.e. over the variable y in the limits from $-a(x)$ to $a(x)$. Integrals of type $\int_{-a}^{a} \rho\, v_x \,\mathrm{d}y$ are replaced by an approximate value:

$$\int\limits_{-a(x)}^{a(x)} \rho(x,y)\, v_x(x,y)\,\mathrm{d}y \approx 2\,a(x)\;\tilde{\rho}(x)\;\tilde{v}_x(x)\,, \tag{7}$$

where $\rho(x,y)$, $v_x(x,y)$ – real plasma density and velocity in the current sheet, $\tilde{\rho}(x)$, $\tilde{v}_x(x)$ – quantities averaged over the thickness of the sheet.

We assume also that the half-thickness a, the velocity of plasma inflowing into the sheet v, the y-component of magnetic field near the current sheet $B_{y\,\mathrm{out}}$, and x- and y-components of magnetic field inside the sheet $B_{x\,\mathrm{in}}$, $B_{y\,\mathrm{in}}$ are small values in comparison with current-sheet half-width b, velocity of plasma outflowing V, and x-component of magnetic field outside the sheet $B_{x\,\mathrm{out}}$. The quantities a and $B_{y\,\mathrm{out}}$ are assumed to change slowly with the x coordinate:

$$\begin{aligned} &a \ll b\,,\\ &v \ll V\,,\\ &B_{y\,\mathrm{out}},\;\; B_{x\,\mathrm{in}},\;\; B_{y\,\mathrm{in}} \ll B_{x\,\mathrm{out}},\\ &\frac{\mathrm{d}\,a}{\mathrm{d}\,x} \ll 1, \qquad \frac{\mathrm{d}\,B_{y\,\mathrm{out}}}{\mathrm{d}\,x} \ll \frac{B_{x\,\mathrm{out}}}{b}. \end{aligned} \tag{8}$$

Hence we can neglect the terms $\sim a^2,\; v^2$ and so on.

A set of equations resulting from the integration and the account of (8) is:

$$\frac{\mathrm{d}}{\mathrm{d}\,x}\;(\rho\, V a) = -\rho_0\, v, \tag{9}$$

$$\frac{\mathrm{d}}{\mathrm{d}\,x}\;\left[V a\left(\rho\,\frac{V^2}{2}+\frac{5}{2}\,p\right)\right] = -v\;\left(\frac{5}{2}\,p_0+\frac{B_x^2}{4\pi}\right) - \\ -\mathscr{S}\,(T,\,n_\mathrm{e},\,n)\,a, \tag{10}$$

$$\frac{\mathrm{d}}{\mathrm{d}\,x}\;\left(\rho\, V^2\, a\right) = -a\,\frac{\mathrm{d}\,p}{\mathrm{d}\,x}+\frac{B_x B_y}{4\pi}\,, \tag{11}$$

$$p = p_0+\frac{B_x^2}{8\pi}\,, \tag{12}$$

$$-\frac{cB_x}{4\pi\, a} = \sigma\;\left(E_0+\frac{1}{c}\,V\,B_y\right). \tag{13}$$

Here (9) is the continuity equation, (10) – the equation of energy conservation; (11) and (12) – the equations of momentum conservation along x- and y-axis, respectively; (13) – Ohm's law. Eq. (11) shows that the hydrodynamic plasma acceleration inside the current sheet along the x-axis is simultaneously due to the gas pressure gradient and to the magnetic field line tension.

The five Eqs. (9)–(13) contain the following five unknown functions: $a(x)$ – half-thickness of the current sheet, $V(x)$ – velocity of plasma outflowing from the RCS, $\rho(x)$ – density of plasma inside the RCS, $T(x)$ – its temperature, $B_y(x)$ – transverse component of magnetic field inside the RCS.

We shall consider the first quadrant of the coordinate plane, assuming the reconnection process to be symmetrical.

For closing the set, the following functions are postulated to be known. $B_x(x)$ – the x-component of magnetic field on the inflow sides of the current sheet – as the first approximation, equals to that in the vicinity of a thin neutral current sheet by Syrovatskii (1971):

$$B_x(x) = -h_0\sqrt{b^2-x^2}\,. \tag{14}$$

Here h_0 is a gradient of the external magnetic field which is a hyperbolic neutral 'point' – the line along the z axis. Velocity $v(x)$ of plasma inflowing into the current sheet is postulated as y-component of the plasma drift velocity to the RCS:

$$\boldsymbol{v}(x) = c\,\frac{\boldsymbol{E}_0\times\boldsymbol{B}}{B^2} \approx c\,\frac{E_0}{B_x}\,\boldsymbol{e}_y\,. \tag{15}$$

Here c is the light speed, $\boldsymbol{E}_0 = E_0\,\boldsymbol{e}_z$ is the external electric field.

In Eq. (10) the radiative loss function

$$\mathscr{S}\,(T,\,n_\mathrm{e},\,n) = n_\mathrm{e} n\,L(T), \tag{16}$$

here n_e is the electron number density; $n = n_\mathrm{H} + n_\mathrm{p}$ – the total number density, consisting of the number density of neutral atoms and ions of hydrogen (e.g., Shmeleva & Syrovatskii 1973); $L(T)$ is the 'normalized' radiative loss function (Cox & Tucker 1969; Raymond et al. 1976; Mewe et al. 1986).

The plasma density ρ_0 and the pressure p_0 outside the current sheet are assumed to be constant. The conductivity of plasma inside the sheet is the ordinary collisional conductivity

$$\sigma = \sigma_0\, T^{3/2}. \tag{17}$$

The pressure $p(x)$ and the temperature $T(x)$ inside the current sheet are connected by the ideal gas ratio:

$$T = \frac{p}{2n_\mathrm{e}k_\mathrm{B}} = \frac{m_\mathrm{i}}{k_\mathrm{B}}\,\frac{p}{2\rho}\,, \tag{18}$$

where m_i is the ion mass, k_B is the Boltzmann constant. For simplisity, we assume here that $m_\mathrm{i} = m_\mathrm{p}$ and $T_\mathrm{e} = T_\mathrm{i} = T_\mathrm{p} = T$ which is reasonable for cold dense current sheets but is not the case of high-temperature turbulent current sheets (Somov 1992).

The boundary conditions for the obtained closed set of Eqs. (9)–(18) ensue from the problem symmetry and are of the form:

$$V(0) = 0, \tag{19}$$

and

$$B_y(0) = 0. \tag{20}$$

The conditions are compatible with the input set of equations.

3. Solving the problem

3.1. Dimensionless form of the problem

The set of Eqs. (9)–(13) can be rewritten for dimensionless functions. The only independent variable x and all functions are devided by their characteristic values, and the dimensionless variables are marked by an asterisk:

$$x^* = \frac{x}{b}\,; \tag{21}$$

$$a^* = \frac{a}{a_0}\,, \quad a_0 = \frac{c^2}{4\pi\,\sigma_0 T_0^{3/2}\,V_\mathrm{d}}\,, \quad V_\mathrm{d} = c\,\frac{E_0}{B_0}\,; \tag{22}$$

$$V^* = \frac{V}{V_\mathrm{A}}\,, \quad V_\mathrm{A} = \frac{B_0}{\sqrt{4\pi\,\rho_0}}\,, \quad B_0 = h_0\,b\,; \tag{23}$$

$$\rho^* = \frac{\rho}{\rho_0}\,, \quad T^* = \frac{T}{T_0}\,; \tag{24}$$

$$p^* = \frac{p}{p_\mathrm{m}}\,, \quad p_\mathrm{m} = \frac{B_0^2}{8\pi}\,; \tag{25}$$

$$B_y^* = \frac{B_y}{\varepsilon\,B_0}\,, \quad \varepsilon = \frac{V_\mathrm{d}}{V_\mathrm{A}}\,; \tag{26}$$

$$B_x^* = \frac{B_x}{B_0}\,, \quad v^* = \frac{v}{V_\mathrm{d}}\,, \quad L^* = \frac{L}{L_\mathrm{max}}\,. \tag{27}$$

Here a_0 is the characteristic value of the current sheet half-thickness; B_0, p_m, V_A, and V_d are the characteristic values of magnetic field, magnetic pressure, Alfvén velocity, and drift velocity outside the current sheet, respectively; L_max is the maximum value of the radiative loss function $L(T)$, $L_\mathrm{max} = 10^{-21}$ erg cm^3 s^{-1}; T_0 is a parameter that will be explained below.

Therefore, the dimensionless equations, that can be obtained in such a way, depend on four free parameters. Two of them – dimensionless α and β – are present in the analogous problem which does not take into account radiative losses (see Sect. 3.4 in Somov 1992).

The first parameter α characterizes the velocity of magnetic reconnection:

$$\alpha = \frac{a_0}{b}\,\frac{V_\mathrm{A}}{V_\mathrm{d}}. \tag{28}$$

Here V_d is the characteristic velocity of plasma drift to the current sheet (see Eq. (22)). In the stationary case under consideration V_d is equal to the velocity of reconnection in the current sheet. The larger velocity V_d into the RCS, the smaller parameter α, and vice versa.

The second parameter β is the ratio of external gas pressure to magnetic one:

$$\beta = \frac{p_0}{p_\mathrm{m}} = \frac{8\pi\,p_0}{B_0^2}\,. \tag{29}$$

This parameter is small if magnetic field outside the RCS is strong enough (see Somov and Syrovatskii 1976a).

The other two parameters – the dimensional value T_0 and dimensionless α_r – have appeared in connection with radiative losses by introducing the dimensional radiative loss function $L(T)$ into the equation of energy conservation (10):

$$T_0 = \frac{B_0^2\,m_\mathrm{i}}{16\pi\,k_\mathrm{B}\,\rho_0}\,, \quad \mathrm{K}\,; \tag{30}$$

and

$$\alpha_\mathrm{r} = \frac{L_\mathrm{max}}{L_0}\,, \quad L_0 = \frac{\sigma_0 T_0^{3/2}\,E_0^2\,m_\mathrm{i}^2}{2\rho_0^2}\,, \quad \mathrm{erg\,cm^3\,s^{-1}}. \tag{31}$$

The characteristic temperature T_0 estimates the temperature of the current sheet without radiative losses. α_r evaluates the role of radiative losses in the modeled current sheet. The larger value α_r, the larger role of radiative losses.

3.2. Input equations

Considering (14), (15), and the boundary condition (19), we integrate Eqs. (9), (10), and (11). After algebraic transformations, we have two dimensionless equations:

$$\frac{\mathrm{d}\,V^*}{\mathrm{d}\,x^*} = \frac{1}{A^2(x^*)\,V^*}\,\left[\sqrt{1-x^{*2}}\,A\,(x^*) - \right.$$

$$-\frac{\alpha\,(1-x^{*2})\,V^*\,\rho^{*5/2}}{\left(1+\beta-x^{*2}\right)^{3/2}} + \frac{x^*A^2(x^*)}{\rho^*} -$$

$$\left. -\frac{A\,(x^*)V^{*2}}{\sqrt{1-x^{*2}}}\right]\,, \tag{32}$$

$$\frac{1}{\alpha A\,(x^*)}\,\rho^*\int\limits_0^{x^*}\alpha_\mathrm{r}\,L^*\,\rho^*\,\frac{A\,(x^*)}{V^*}\,\mathrm{d}\,x^* -$$

$$-\rho^*\,\left(\frac{5}{2}\,\beta + 1 + \frac{x^*\,\sqrt{1-x^{*2}}}{A\,(x^*)} - V^{*2}\right) +$$

$$+\frac{5}{2}\,(1+\beta-x^{*2}) = 0. \tag{33}$$

Here $A\,(x^*) \equiv \arcsin x^*$. The equations contain parameters α, β, T_0, and α_r. Using these equations, the functions $V^*(x^*)$ and $\rho^*(x^*)$ can be found.

Further, the remaining unknown functions $T(x^*)$, $B_y^*(x^*)$, and $a^*(x^*)$ can be calculated from the following analytical expressions:

$$T^*(x^*) = \frac{1+\beta-x^{*2}}{\rho^*}\,, \qquad T(x^*) = T_0\,T^*(x^*), \tag{34}$$

$$B_y^*(x^*) = -\frac{1}{V^*} - \alpha\,\rho^*\,\frac{\sqrt{1-x^{*2}}}{A(x^*)\,T^{*3/2}}\,, \tag{35}$$

$$a^*(x^*) = \frac{A(x^*)}{\alpha\,\rho^*\,V^*}\,. \tag{36}$$

3.3. Taylor series expansion

The velocity V^* of plasma outflowing from the current sheet is determined from the differential Eq. (32) if the density ρ^*, needful for the computations, can be found from the integral Eq. (33). To solve both equations numerical methods are necessary. However the right-hand side of (32) and also some terms in (33) become the indeterminate forms of type 0/0 when $x^* \to 0$. So, direct numerical methods are not applicable in the vicinity of the point $x^* = 0$.

In order to avoid this difficulty, the functions $V^*(x^*)$ and $\rho^*(x^*)$ for small x^* have to be calculated by using the Taylor series expansion

$$f(x) \approx f(0) + f^{(1)}(0)\, x + \frac{1}{2!}\, f^{(2)}(0)\, x^2 + \ldots \qquad (37)$$

and for x^* larger than a certain value x_1^* – directly from Eqs. (32) and (33). The coefficients of the expansion $V^*(0)$, $\rho^*(0)$, $V^{*(1)}(0)$, $\rho^{*(1)}(0)$, ..., $V^{*(5)}(0)$, $\rho^{*(5)}(0)$ have to be obtained by the following manner. Eqs. (32) and (33) are successively differentiated, the indeterminate forms are evaluated by using Lopital's rule, and, as a result, equations for the sought coefficients are derived. These equations have been solved numerically.

4. Numerical results

4.1. Selection of parameters

Numerical computations have been performed for the following parameters:

α = 0.01, 0.1, 1.28, and 12;
β = 0.1;
T_0 = $5\,10^4$ and $5\,10^8$ K;
$\alpha_{\rm r}$ = 0.1 and 1.

Parameter β is not changed because the solution does not practically depend on it (Somov 1992). Parameter α values are taken the same that in (Somov 1992) for convenience of comparison. Values T_0 are chosen so that current sheet temperatures computed are of order 10^4 and 10^8 K, i.e. at the boundaries of the interval over which the radiative loss function is known. The value $\alpha_{\rm r} = 0.1$ describes the case when the role of radiative cooling is small; $\alpha_{\rm r} = 1$ increases an influence of radiative cooling.

For each value of the parameter α and for the fixed value $\beta = 0.1$ the following pairs of the parameters, describing the radiation, are set:

(a) $T_0 = 5\,10^4$ K, $\alpha_{\rm r} = 0.1$;
(b) $T_0 = 5\,10^4$ K, $\alpha_{\rm r} = 1$;
(c) $T_0 = 5\,10^8$ K, $\alpha_{\rm r} = 1$.

These pairs of the parameters correspond to: (a) the 'cold' current sheet with a small role of radiative cooling, (b) the 'cold' current sheet with a large role of radiative cooling, (c) the 'super-hot' current sheet with a large role of radiation but without heat conduction. The last case might be, in principle, a part of high-temperature RCS with closed field lines – a 'magnetic island'. So, the twelve models could be computed in general.

Variants (a) and (b), corresponding to the 'cold' current sheet ($T_0 = 5\,10^4$ K), are computed without problems. Difficulties appear when the structure of the 'super-hot' current sheet ($T_0 = 5\,10^8$ K) is computed. Formally, in the case (c), solutions show a sensitivity to changing x_1^*: small variations of x_1^* lead to significant changes in $V^*(x^*)$ and $\rho^*(x^*)$.

Therefore, only eight variants from twelve mentioned above are reliable – those (a) and (b) corresponding to the 'cold' current sheet. They will be described in Sect. 4.2. The possible causes of instability of solutions for 'super-hot' current sheet (c) will be discussed in Sect. 4.3.

4.2. Cold current sheet

(a) The case $\alpha_{\rm r} = 0.1$ means a small role of radiative losses in energy balance of the RCS. According to our computations, the solution of the problem in this case differs only slightly from the idealized solution (see Somov 1992) when radiative losses are not taken into account. The deviation is insignificant on a scale of Figs. 2-4 which show the idealized solution ($L(T) \equiv 0$) by dashed curves. Numbers near the curves indicate the corresponding values of parameter α that are the same as in Somov (1992) for conveniency of comparison. This allows us to conclude that the numerical method (see Appendix) under use works well enough.

(b) The solutions with the parameters $T_0 = 5\,10^4$ K and $\alpha_{\rm r} = 1$ are shown in Figs. 2-4 by solid curves.

Fig. 2 shows that the velocity V^* of plasma outflowing from the current sheet is smaller as compared with that in the idealized case $L(T) \equiv 0$. It is associated with the fact that now not all energy inflowing in the sheet outflows from it as kinetic energy of plasma, but a part of energy is radiated. As a consequence, density ρ^* of plasma becomes larger, especially in the center region of the current sheet. The temperature T (see Fig. 3) is smaller than in the idealized case.

Fig. 4 demonstrates that the transverse component of magnetic field B_y^* strongly depends on parameter α. For $L(T) \equiv 0$ and $\alpha > 1.28$ (i.e. at small velocities of reconnection), the transverse component B_y^* changes the sign from positive to negative in some point x^*, that is a 'magnetic island' – region of closed field lines – appears in the center part of the current sheet (Fig. 5b). When radiative losses are taken into account, a 'magnetic island' appears already at $\alpha = 0.1$, i.e. there, where it is absent at $L(T) \equiv 0$.

We believe that this solution makes more probable the formation of quiescent prominences as a result of slow magnetic reconnection in the RCS with magnetic island in the central region of current sheet. Here the cold dense plasma may be accumulated creating a large filament.

4.3. Super-hot current sheet

The sensitivity of the solutions obtained for the 'super-hot' current sheet ($T_0 = 5\,10^8$ K) to changing x_1^* can be interpreted as the absence of its stable states under given conditions. Thermal instability can be a cause of this phenomenon.

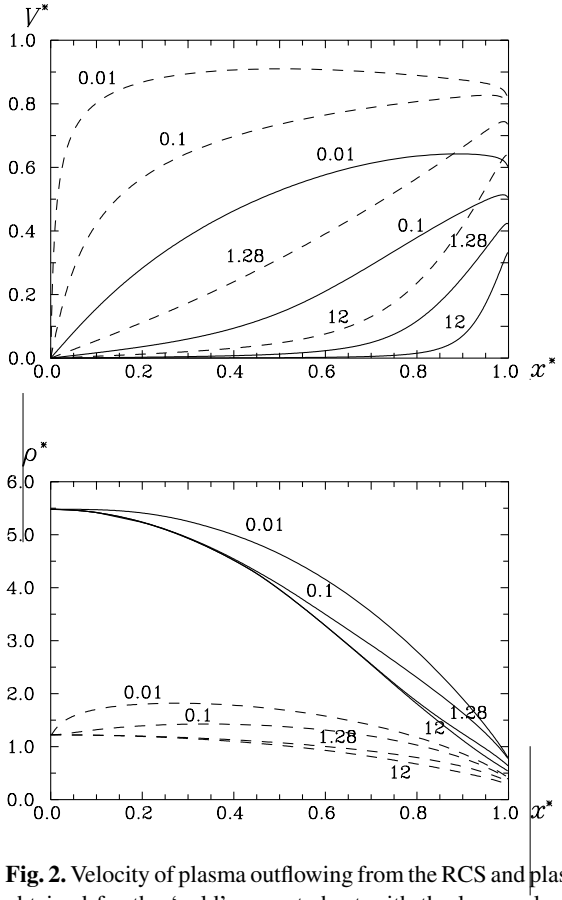

Fig. 2. Velocity of plasma outflowing from the RCS and plasma density obtained for the 'cold' current sheet with the large role of radiative losses (solid lines) and results for the case when radiative losses are not taken into account (dashed lines). Numbers near the curves indicate the values of parameter α

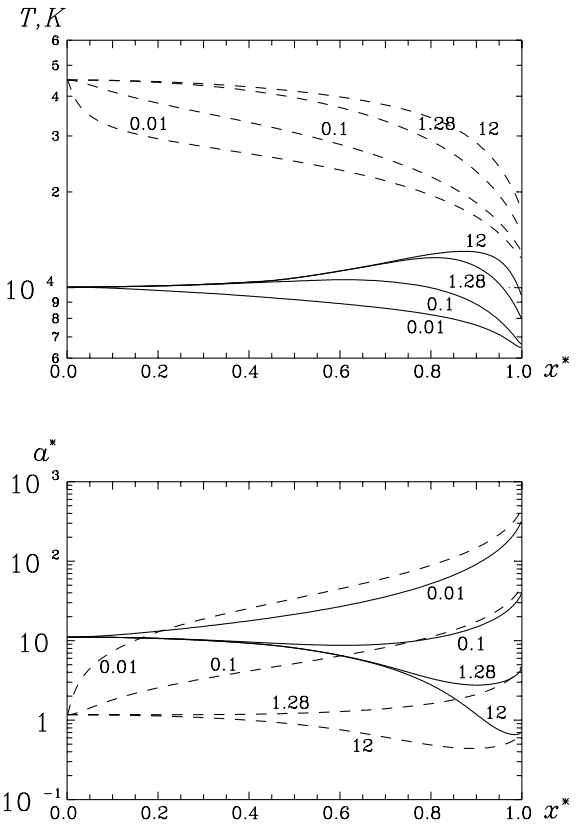

Fig. 3. Plasma temperature and thickness of the RCS obtained for the 'cold' current sheet with the large role of radiative losses (solid lines) and results for the case when radiative losses are not taken into account (dashed lines). Numbers near the curves indicate the values of parameter α

A linear theory of thermal instability was developed by Field (1965) (see also Somov & Syrovatskii, 1976b). According to this theory, homogeneous medium, which is in thermal and mechanical equilibrium, is characterized, in particular, by a certain parameter δ. In the case when: (i) the energy inflowing per 1 g of substance per 1 s does not depend on temperature and density, and (ii) cooling is determined by radiative losses (16), the parameter δ is

$$\delta = \frac{\mathrm{d}\,\ln L}{\mathrm{d}\,\ln T}\,. \tag{38}$$

There exist the temperature ranges where small perturbations of the following types are unstable:

1. Perturbations with p = const are unstable in the ranges with $\delta < 1$; this is the so-called *condensation* mode of the thermal instability.
2. Perturbations with constant entropy grow in the temperature ranges where $\delta < -3/2$; this corresponds to the *sound* or *wave* mode.
3. Perturbations with n = const; they are unstable in the ranges with parameter $\delta < 0$.

The dependence $\delta(T)$ within the temperature range from $8.5\,10^3$ to $1.8\,10^8$ K has been computed using function $L(T)$ from Cox & Tucker (1969). The result is that the parameter $\delta < 1$ in two temperature ranges: $2\,10^4 - 3.5\,10^4$ K and $9\,10^4 - 1.8\,10^8$ K. Therefore, the thermal instability can take place in a 'super-hot' current sheet with temperature $T \sim 10^8$ K, if heat conduction is supressed somehow.

Generally speaking, this conclusion seems to be reasonable for the conditions described above but it is not entirely valid for the current sheet model considered. First of all, this is because the plasma inside the RCS is not homogeneous ($\rho \neq$ const) and is not in the statical equilibrium ($V \neq$ const) in our problem. Nevertheless, in the first approximation, the instability obtained in the computations of the current sheet structure at $T \sim 10^8$ K may be attributed to the thermal instability. As known, the thermal instability in the RCS can be well stabilized by heat conduction (Somov & Syrovatskii 1982). The investigation of this problem conformably to the model described above will be the object of the next paper (Paper 2).

5. Discussion and conclusion

Modeling an equilibrium state of the reconnecting current sheet was the object of the study of many papers starting from Heyvaerts & Priest (1976), Syrovatskii (1976b), Smith & Priest

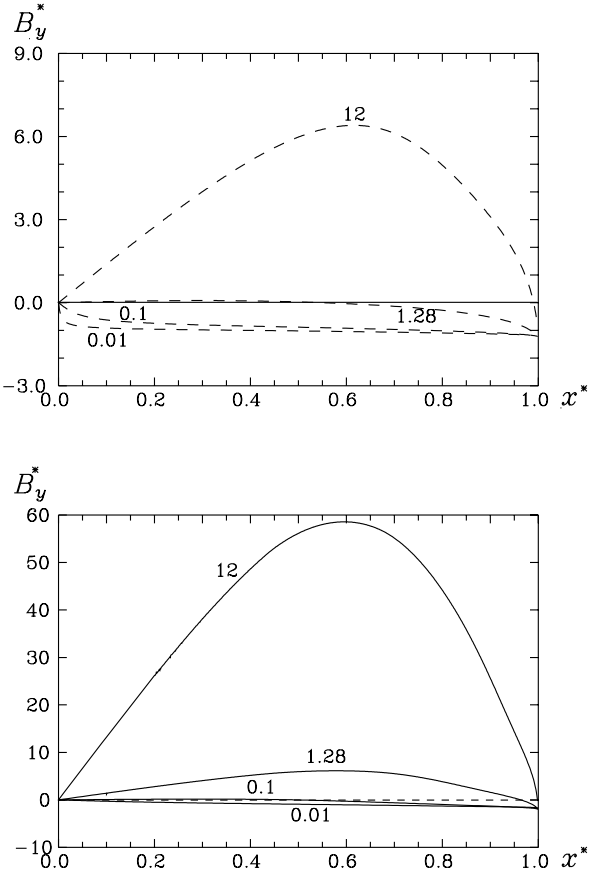

Fig. 4. Transverse magnetic field in the RCS obtained for the 'cold' current sheet with the large role of radiative losses (solid lines) and results for the case when radiative losses are not taken into account (dashed lines). Numbers near the curves indicate the values of parameter α

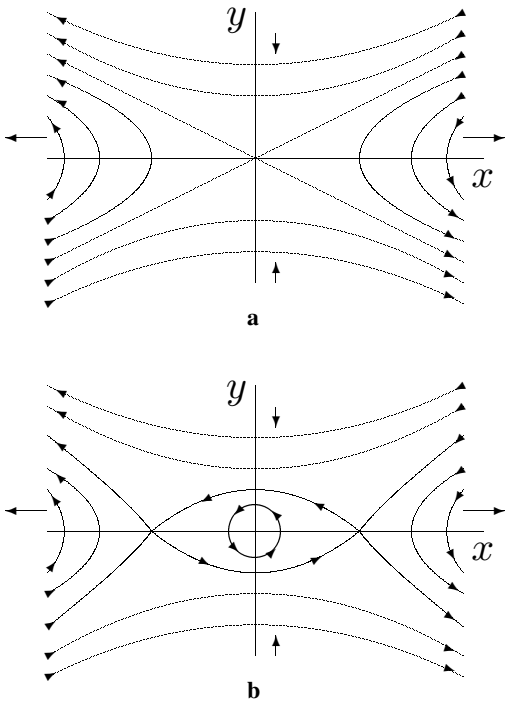

Fig. 5a and b. Configurations of magnetic field in the reconnecting current sheet: **a** X-type – fast regime of reconnection, $\alpha \ll 1$; **b** O-type ('magnetic island') – slow regime of reconnection, $\alpha \gg 1$

(1977). The basic method consists in that the plasma parameters inside the RCS (such as an average temperature, density, pressure, and others) are determined via the parameters of an external plasma, the external electric and magnetic field strength by using the steady MHD equations as the order-of-magnitude relations. For simplicity, the current sheet is supposed to be magnetically neutral, i.e. the external magnetic field lines are parallel to the sheet surface, and there is not any magnetic field inside the RCS. Besides, the current sheet is considered as a whole, i.e. all the values, characterising it, do not depend on spatial coordinates.

The main conclusion by Syrovatskii (1976b) is that, under definite conditions in the external plasma, the temperature of the RCS becomes equal to certain critical value ($\approx 8\,10^4$ K). At this point, the radiative losses cannot balance the Joule heating, and the temperature of the RCS should rapidly begin to rise. The RCS evolves towards a new, more hot, equilibrium state. The rapid heating of the RCS can lead to a chain of kinetic processes in the plasma: a break of the electron temperature, development of ion-acoustic or Buneman instability; plasma becomes turbulent. Because the RCS is not homogeneous in actual conditions, these processes have a local character. As a result, a break of the RCS occurs, that can be identified with the onset of the explosive phase of a flare.

Current sheets modeled by Heyvaerts & Priest (1976) do not differ too much from that of Syrovatskii (1976b) at low temperatures. The thermal equilibrium of the RCS and its possible evolution is studied. The RCS is considered which forms between the new flux emerging from under the solar photosphere and a preexisting magnetic field. The height of the RCS over the photosphere increases with time. All parameters of external plasma are given as functions of height h, i.e. some model of the atmosphere is adopted. As a result, the current sheet temperature is computed at various heights for two atmosphere models: weakly convective and strongly convective. A conclusion is made that with increasing h the RCS heats, remaining nevertheless colder than ambient plasma. However, when it attains certain critical height, the low-temperature thermal equilibrium becomes impossible, and the RCS rapidly heats, seeking a new equilibrium state. During this process current-driven instability may be triggered, resistivity is enhanced, electric field is induced that results in generating high-energy particles. The impulsive phase of solar flares can be interpreted in such a way. As seen, the conclusion, in general, agrees with that of Syrovatskii (1976b) but the critical temperature is slightly lower ($\approx 10^4$ K).

Smith & Priest (1977) consider the RCS in the lower corona or upper chromosphere. Movement of the plasma inside and outside the RCS is not taken into account. An assumption is also made that the current sheet is enough thick, so Joule heating and the heat conduction across it are insignificant. The temper-

ature of the RCS is calculated as a function of its length L. It is shown that if the length increases up to certain value $L_{\max}$, then the equilibrium becomes unstable and the RCS cools down until it achieves a new stable state. In this way, Smith & Priest demonstrate a possibility of forming the quiescent prominences by thermal instability in a current sheet. In fact, for the first time, Smith & Priest argue that quiescent prominences may 'for good theoretical reasons' form in current sheet. All three models mentioned above do not consider the structure of the RCS.

A model of Milne & Priest (1981) compares favourably with those mentioned above, first of all because it studies an internal structure of RCS. More exactly, variations of plasma parameters along the thickness of the sheet at the centre of symmetry are investigated. As formerly, the current sheet is assumed to be magnetically neutral, with the temperature $T \leq 10^6$ K. It appears that the solution depends, in particular, on two dimensionless parameters. The first, β, is equal to the ratio of gas pressure to magnetic one outside the RCS (see our (29)). The second, r, is the ratio of the radiative loss term to the convective term in the energy equation. If β or r is too small, no solution exists. The spatial profiles of the inflow speed, density, and magnetic field inside the sheet are computed for various values of β and fixed $r = 1.2\,10^{-2}$. It has been shown that as β decreases towards its cut-off value the profiles steepen locally towards a step function. The results are applied to the emerging flux model for solar flares. As the current sheet rises through the solar atmosphere the value β decreases, magnetic field gradient increases and a threshold value of the current density $j_{\rm crit}$, beyond which turbulent behaviour ensues, may be exceeded. The RCS now heats up, seeking a new equilibrium state. The critical height decreases with increasing magnetic field strength.

We develop a new model of a reconnecting current sheet. It differs from other analogous models, first of all, in that the magnetic field inside the RCS has the transverse component $B_\perp \neq 0$, i.e. the current sheet is magnetically non-neutral. Moreover, we study a longitudinal structure of the RCS, i.e. variations of the plasma parameters along its width.

Our model describes both the slow regime of reconnection, when the magnetic field configuration of O-type forms – the so-called 'magnetic island' in the central part of the RCS, and fast regime with configuration of X-type. Particular attention is given to influence of radiative losses on the current sheet structure. Models for 'cold' ($T \sim 10^4$ K) and 'superhot' ($T \sim 10^8$ K) current sheets have been computed. The cold current sheet is found to be thinner, denser, colder, with smaller velocity of plasma outflowing from it as compared with the case when radiative losses are not taken into account. Existence of the slow regime of reconnection may interpret the formation of quiescent prominences in the solar corona. Indeed, at the low velocities plasma flows into the current sheet with magnetic configuration of O-type and is found to be practically blocked up in the magnetic island. Its density increases with time that results in increasing the radiative losses $n_{\rm e}^2\,L(T)$, and consequently in cooling the plasma. Our general conclusion that prominences may arise due to magnetic reconnection in current sheets is in agreement with that of Smith & Priest (1977); however, as mentioned above, proposed mechanisms of such a process are different. The transition from the slow reconnection (with the configuration of O-type) to the fast one (with the configuration of X-type) presumably means destabilization of a quiescent prominence and triggering a solar flare.

Taking into account radiative losses in the case of the 'superhot' current sheet leads to absence of its stable states. It can be related to the development of thermal instability at $T \sim 10^8$ K under condition when heat conduction is prohibited for some reason. This may be, for example, the case of high-temperature 'plasmoid' formation during a solar flare. As known, the thermal instability of the RCS can be stabilized by heat conduction (Somov & Syrovatskii 1982). The investigation of this problem conformably to the model described above will be the object of the next paper.

Acknowledgements. This research was partially supported by the Russian Fund of Fundamental Reasearches (Grant 96-02-18055). One of the authors (B. V. S.) would like to thank the National Astronomical Observatory of Japan (NAOJ) for inviting him as a guest professor (1996 - 1997) and providing him with the financial support; this work has been supported by a Grant-in-Aid for Science Research from the Ministry of Education, Science, Sports and Culture (No. 08304021). He also feels grateful to his colleagues for very friendly and generous hospitality during his work in NAOJ and stay in Japan.

Appendix A: numerical method

(1) For small x^* the velocity $V^*(x^*)$ of plasma outflowing from the RCS and density $\rho^*(x^*)$ are calculated by means of the Taylor series expansion. So, boundary condition for differential Eq. (32) may be determined at some point x_1^*: $V_1^* = V^*(x_1^*)$.

(2) For x^* larger certain x_1^* the function $V^*(x^*)$ is computed directly from Eq. (32) by using the Rungue-Kutt method. This method compares favourably with others. Indeed, let us consider, as example, an ordinary differential equation:

$$\frac{\mathrm{d}\,y}{\mathrm{d}\,x} = f(x, y)\,. \tag{A1}$$

Then (i) the method is one-stepped: to obtain y_{m+1} an information only on a previous point (x_m, y_m) is needful; (ii) calculating the derivatives of $f(x, y)$ is not required, only a calculation of $f(x, y)$ is needed. The disadvantage is that to calculate one subsequent point of the solution, the function $f(x, y)$ has to be calculated several times for various values x and y. Thus, the working formulae are

$$y_{m+1} = y_m + \frac{h}{6}\,(k_1 + 2\,k_2 + 2\,k_3 + k_4), \tag{A2}$$

where

$$k_1 = f(x_m,\, y_m), \tag{A3}$$

$$k_2 = f\left(x_m + \frac{h}{2},\, y_m + \frac{h\,k_1}{2}\right), \tag{A4}$$

$$k_3 = f\left(x_m + \frac{h}{2},\, y_m + \frac{h\,k_2}{2}\right), \tag{A5}$$

$$k_4 = f(x_m + h,\, y_m + h\,k_3), \tag{A6}$$

and h is the step of computation. So, the function $y = y(x)$ can be determined for any x using known (x_1, y_1).

(3) Note, that to calculate the right-hand side of Eq. (32), function $\rho^*(x^*)$ has to be known. Its values are determined from Eq. (33), where the integral is replaced by the formula of trapezium, namely:

$$F(x_{m+1}) \equiv \int_0^{x_{m+1}} f(x)\,\mathrm{d}\,x \approx \tag{A7}$$

$$\approx F(x_m) + \frac{1}{2}\,[f(x_m) + f(x_{m+1})]\,(x_{m+1} - x_m).$$

So, Eq. (33) becomes algebraical and can be solved, for example, using method of dividing an segment in half.

(4) To compute the under-integral function

$$f(x^*) = \frac{L(T)}{L_0}\,\rho^*(x^*)\,\frac{A(x^*)}{V^*(x^*)}, \tag{A8}$$

the value of tabularly given function $L(T)$ has to be calculated in any point $T = T(x^*)$. On this purpose, Eitken's linear interpolation algorithm is used. Let $y(x)$ be given tabularly in an irregular grid (x_1, y_1), $(x_2, y_2), \ldots, (x_n, y_n)$; x is the point at which the value y has to be determined. Then two points x_a and x_b are chosen so that $x_a \leqq x \leqq x_b$ and y is obtained from the expression

$$y = \frac{y_a\,(x_b - x) + y_b\,(x_a - x)}{x_b - x_a}. \tag{A9}$$

References

Biskamp D., 1986, Phys. Fluids 29, 1520

Biskamp D., 1993, Nonlinear Magnetohydrodynamics. Cambridge University Press, Cambridge

Brushlinskii K.V., Zaborov A.M., Syrovatskii S.I., 1980, Soviet J. Plasma Phys. 6, 165

Cox D.P., Tucker W.H., 1969, ApJ 157, 1157

Field G.B., 1965, ApJ 142, 531

Forbes T.G., Priest E.R., 1982, Solar Phys. 81, 303

Forbes T.G., Priest E.R., 1983, Solar Phys. 84, 169

Forbes T.G., Acton L.W., 1996, ApJ 459, 330

Giovanelli R.G., 1946, Nat 158, 81

Hesse M., Birn J., Baker D.N., Slavin J.A., 1996, JGR 101, No. A5, 10805

Heyvaerts J., Priest E.R., 1976, Solar Phys. 47, 223

Hones E. W. Jr. (ed.) 1984, Magnetic Reconnection in Space and Laboratory Plasmas. Amer. Geophys. Un., Washington

Kosugi T., Makishima K., Murakami T., et al., 1991, Solar Phys. 136, 17

Kosugi T., Somov B.V., 1997. In: Watanabe T., Kosugi T., Sterling A. (eds.) Proc. Yohkoh Fifth Anniversary Symposium on 'Observational Plasma Astrophysics: Five Years of Yohkoh and Beyond', in press.

Masuda S., Kosugi T., Hara H., Tsuneta S., Ogawara Y., 1994, Nat 371, 495

Masuda S., Kosugi T., Hara H., et al., 1995, PASJ 47, 677

Mewe R., Lemen J., van den Oord, G.H.J., 1986, A&AS, 63, 511

Milne A.M., Priest E.R., 1981, Solar Phys. 73, 157

Ogawara Y., Takano T., Kato T., Kosugi T., et al., 1991, Solar Phys. 136, 1

Petschek H.E., 1964. In: Hess W. N. (ed.), AAS-NASA Symp. on the Physics of Solar Flares, NASA SP-50, p.425

Podgorny A.I., Syrovatskii S.I., 1981, Soviet J. Plasma Phys. 7, 580

Priest E.R., Lee L.C., 1990, J. Plasma Phys. 44, 337

Raymond J.C., Cox D.P., Smith B.W., 1976, ApJ, 204, 290

Shmeleva O.P., Syrovatskii S.I., 1973, Solar Phys. 33, 341

Smith E.A., Priest E.R., 1977, Solar Phys. 53, 25

Somov B.V., 1992, Physical Processes in Solar Flares. Kluwer Academic Publ., Dordrecht, Holland

Somov B.V., 1994, Fundamentals of Cosmic Electrodynamics. Kluwer Academic Publ., Dordrecht, Holland

Somov B.V., Syrovatskii S.I., 1976a. In: Basov N.G. (ed.) Neutral Current Sheets in Plasmas. New York: Consultants Bureau, vol. 74, p. 13

Somov B.V., Syrovatskii S.I., 1976b, Soviet Physics Usp. 19, 813

Somov B.V., Syrovatskii S.I., 1982, Solar Phys. 75, 237

Sweet P.A., 1969, ARA&A 7, 149

Syrovatskii S. I., 1966, Soviet Astronomy – AJ 10, 270

Syrovatskii S.I., 1971, Soviet Physics – JETP 33, 933

Syrovatskii S.I., 1976a. In: Basov N.G. (ed.) Neutral Current Sheets in Plasmas. New York: Consultants Bureau, vol. 74, p. 1

Syrovatskii S. I., 1976b, Soviet Astron. Lett. 2, 13

Tsuneta S., 1996, ApJ 456, 840

Tsuneta S., Acton L., Bruner M., et al., 1991, Solar Phys. 136, 37

Tsuneta S., Masuda S., Kosugi T., Sato J., 1997, ApJ, 478, 787

Uchida Y., Kosugi T., Hudson H.S. (eds.) 1996, Magnetohydrodynamic Phenomena in the Solar Atmosphere - Prototypes of Stellar Magnetic Activity. Kluwer Academic Publ., Dordrecht, Holland.

This article was processed by the author using Springer-Verlag LaTeX A&A style file *L-AA* version 3.